AIP Applied Physics Letters

Liquid-crystal-based terahertz tunable Lyot filter

Chao-Yuan Chen, Ci-Ling Pan, Cho-Fan Hsieh, Yea-Feng Lin, and Ru-Pin Pan

Citation: Applied Physics Letters **88**, 101107 (2006); doi: 10.1063/1.2181271
View online: http://dx.doi.org/10.1063/1.2181271
View Table of Contents: http://scitation.aip.org/content/aip/journal/apl/88/10?ver=pdfcov
Published by the AIP Publishing

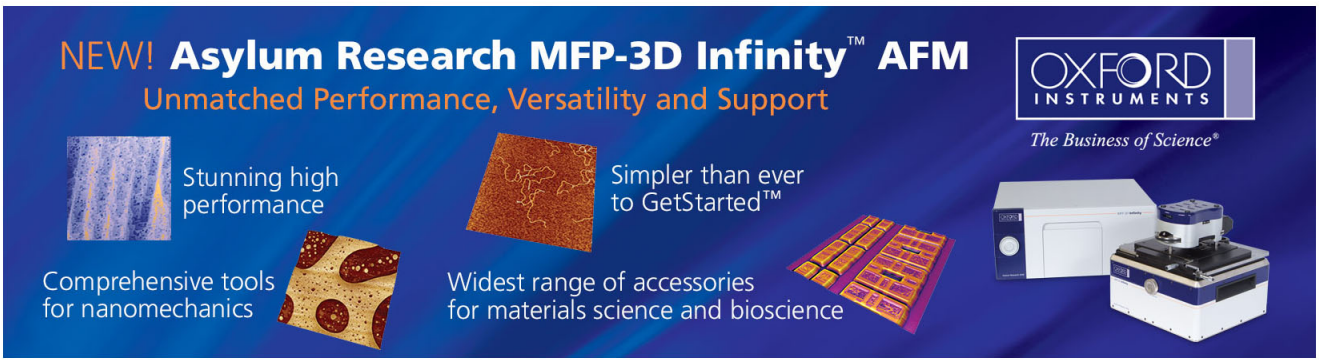

Liquid-crystal-based terahertz tunable Lyot filter

Chao-Yuan Chen and Ci-Ling Pan[a)]
Department of Photonics, Institute of Electro-Optical Engineering, National Chiao Tung University, 1001 Ta Hsueh Road, Hsinchu, Taiwan 30010, Republic of China

Cho-Fan Hsieh, Yea-Feng Lin, and Ru-Pin Pan[b)]
Department of Electrophysics, National Chiao Tung University, 1001 Ta Hsueh Road, Hsinchu, Taiwan 30010, Republic of China

(Received 28 July 2005; accepted 17 January 2006; published online 8 March 2006)

A two-element tunable Lyot filter operating in the terahertz (THz) frequency range is demonstrated. The central bandpass frequency of the filter can be continuously tuned from 0.388 to 0.564 THz (a fractional tuning range of 40%) using magnetically controlled birefringence in nematic liquid crystals. The transmission bandwidth is 0.1 THz and the insertion loss of the present device is 8 dB due to the scattering of LC molecules in the thick LC cells. This filter can be operated at room temperature. © *2006 American Institute of Physics*. [DOI: 10.1063/1.2181271]

For THz studies of ultrafast dynamics in materials to medical, environmental sensing, and imaging as well as[1–3] future applications in THz communication and surveillance, quasi-optic components such as filters, phase shifters, attenuators, and polarizers are indispensable. Up to now, several designs of THz filters have been reported. These include frequency filters such as two-dimensional metallic hole arrays (2D-MHA) or photonic crystals that act as a bandpass filter or frequency selective surface (FSS).[4,5] A filter with fixed center frequency of 0.4 THz using a binary grating with rectangular grooves as FSS was also demonstrated.[6] Wu *et al.* reported a THz plasmonic high pass filter consisting of high-aspect-ratio micron-sized wire arrays.[7] Tunable THz filter designs include: a tunable THz attenuator and filter based on a mixed-type I/type II GaAs/AlAs multiple quantum well structure tuned by optical injection;[8] a metallic photonic crystal filter made tunable over the range of 365–386 GHz by a relative lateral shift of 140 μm between two micromachined metallic photonic crystal plates.[9] By use of $SrTiO_3$ as a defect material inserted into a periodic structure of alternating layers of quartz and high-permittivity ceramic, Nemec *et al.*[10] tuned a single defect mode in the one-dimensional photonic crystal from 185 GHz at 300 K down to 100 GHz at 100 K. Voltage controlled wavelength selection at microwave frequencies was achieved by Yang and Sambles[11] using a structure of metallic slat gratings with the thin grooves between the metallic slats filled with nematic liquid crystal (NLC). Similarly, Tanaka and Sato[12] reported electrically controlled millimeter-wave (up to 94 GHz) transmission properties of stack-layered NLC cells with metal substrates. Recently, we reported control of enhanced THz transmission through 2D-MHA using magnetically controlled birefringence in NLC.[13]

The Lyot filter,[14] a type of birefringent filter widely employed in the visible and near infrared, is based on interference of polarized light a stack of birefringent elements with their optical axes rotated with respect to each other. Lyot filters can be made tunable using active birefringent retarders such as electro-optic crystals[15] and liquid crystal cells.[16] Recently, we have developed variable THz phase shifters or retarders[17,18] by magnetically controlling the birefringence in NLCs.[18–20] In this letter, we construct and characterize a room-temperature tunable THz Lyot filter based on magnetically controlled retardation in liquid crystal (LC).

Two kinds of LC cells, the homogeneous and homeotropical cells, are used in our filter. Each cell is constructed with two fused silica plates with aluminum spacers and filled with E7 (Daily Polymer Crop., Taiwan). The inner silica surfaces of homogeneous cells are coated with polyimide[21] followed by rubbing while the homeotropic cells are coated with *N*,*N*-dimethyl-*n*-octadecyl-3-aminopropyltrimethoxysilyl chloride,[22] to align the LC molecules parallel and perpendicular to the surface, respectively.

The LC-based Lyot filter has two elements, *A* and *B*, which are separated by a linear polarizer (Fig. 1). Each element consists of a fixed retarder (FR) and a tunable retarder (TR). The FR consists of a pair of permanent magnets sandwiching a homogeneously aligned LC cell. Sufficiently large magnetic field is required for quenching the director fluctuation of LC molecules and reducing the scattering in the thick LC cell [inset (a) of Fig. 1]. The homogeneous cells in FR_A and FR_B supply fixed phase retardations, Γ_A and Γ_B, respectively, for THz waves. The tunable retarders, TR_A and TR_B [inset (b) of Fig. 1], are used to achieve the desired variable phase retardation, $\Delta\Gamma_A$ and $\Delta\Gamma_B$. They are of our previous design,[17,18] i.e., a fixed homeotropically aligned LC cell nor-

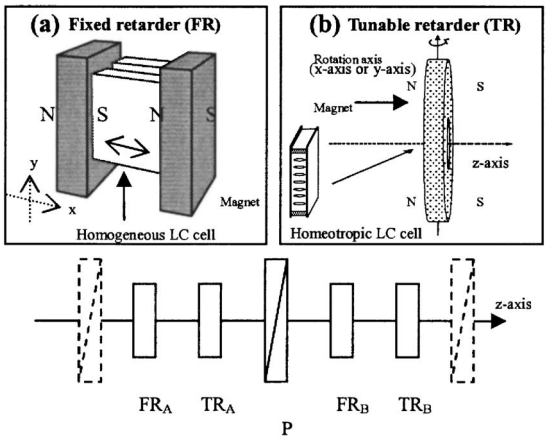

FIG. 1. The schematic diagram of the LC-based tunable THz Lyot filter. P: polarizer; N: North pole; S: South pole.

[a)]Electronic mail: clpan@faculty.nctu.edu.tw
[b)]Electronic mail: rpchao@mail.nctu.edu.tw

mal to the z axis is placed at the center of the magnet rotatable along the x or y axis (see Fig. 1). As the magnet rotates to a new position, the LC molecules are reoriented parallel to the new field direction and provides a variable effective index of refraction.

The transmittance, T, of the two-element Lyot filter for normally incident THz wave can be written as[14]

$$T = \cos^2\left(\frac{\Gamma_A + \Delta\Gamma_A}{2}\right) \cdot \cos^2\left(\frac{\Gamma_B + \Delta\Gamma_B}{2}\right). \quad (1)$$

Because of the birefringence of LC, the THz waves which pass through each element will be separated into extraordinary and ordinary rays (e ray and o ray) with corresponding time delays $\Delta\tau$, and the phase retardation $\Gamma = 2\pi \cdot \Delta\tau \cdot f$. The transmittance of the THz Lyot filter as a function of frequency of the THz waves, f, is then given by

$$T(f) = \cos^2(\pi \cdot \Delta\tau_A \cdot f) \cdot \cos^2(\pi \cdot \Delta\tau_B \cdot f). \quad (2)$$

The Lyot filter in this work is designed such that $\Delta\tau_B = 2\Delta\tau_A$. Satisfying this condition, $T(f)$ in Eq. (2) becomes

$$T(f) = 4\cos^6(\pi \cdot \Delta\tau_A \cdot f) - 4\cos^4(\pi \cdot \Delta\tau_A \cdot f) + \cos^2(\pi \cdot \Delta\tau_A \cdot f). \quad (3)$$

The first maximum of $T(f)$ occurs when the condition $\Delta\tau_A \cdot f = 1$ is fulfilled.

The filter can be operated in either the "positive" or "negative" mode. That is, the corresponding phase retardation provided by the TRs is positive or negative. The frequency tunable range can be extended by operating the filter in both modes. In the positive/negative mode, the rotary axes of the magnets in TR_A and TR_B is parallel to y/x axis. The retardations by the TRs, $\Delta\Gamma_A$ and $\Delta\Gamma_B$, are then both positive/negative with respect to the retardation by the FRs. The angle between the aligned direction of homogeneous cells and the polarization of THz waves is 59°. Discussion about this chosen angle is given later in this letter.

The thicknesses of LC layers in FR_A and FR_B are 4.5 and 9.0 mm each. A pair of permanent magnets (sintered Nd–Fe–B) with the magnetic fields (~0.18 T) parallel to the LC cell surfaces is used in order to ensure stable alignment.[23] The thickness of LC layers in TR_A and TR_B are 2.0 and 4.0 mm, respectively. The maximum magnetic field at cell position in the rotary permanent magnets is 0.427 T. The retardation of THz waves through the homeotropic cells can be tuned by rotating the magnets. TR_A and TR_B can be either positive or negative depending on the rotary axes that are parallel to the y or x axis. The filter was characterized by using a photoconductive-antenna-based THz time-domain spectrometer.[24]

An example of the transmitted THz spectrum through the filter with the $\Delta\tau_A = 2.2$ ps normalized to the maximum of transmittance, is shown in Fig. 2. The transmitted peak frequency and the bandwidth of the filter are 0.465 and ~0.10 THz, respectively. The corresponding THz temporal profile with total retardation, $\Delta\Gamma = 0$ is shown in the inset of Fig. 2. Note that there are four peaks with peak separations equal to $\Delta\tau_A$. This can be understood as follows: The THz wave is separated into o ray and e ray after passing the first element and these two waves are further separated into o-o ray, e-o ray, o-e ray and e-e ray, respectively, again after passing the second element. The transmission spectrum can be considered as a manifestation of the interference among

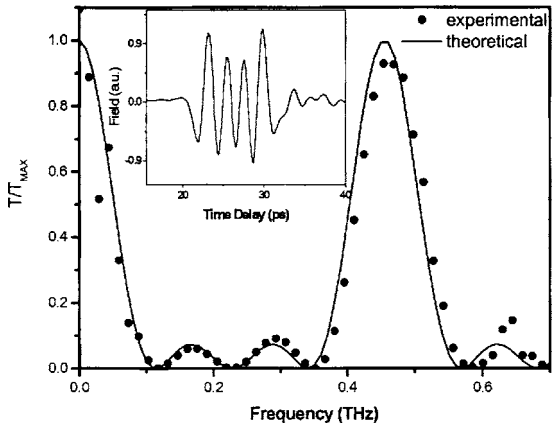

FIG. 2. An example of the transmitted spectrum of the broadband THz pulse through the LC filter. The time-domain signal is shown in the inset.

the four peaks of the THz signal in the time domain. The theoretical curve according to Eq. (2) is shown as the solid curve, which agrees with the experimental data.

The birefringence of E7 estimated from the $\Delta\tau_A$ and the thickness of the LC layer is 0.155 in the sub-THz frequency range. This is somewhat smaller than what we reported previously (0.170).[18] It is also lower than that in the visible but in accord with reported dielectric anisotropy in the microwave and millimeter wave range.[11] Conceivably, the effect of thermal fluctuations of molecular orientations in a LC layer as thick as 9 mm could significantly reduce the effective birefringence of the LC.

The filter is tuned by rotating the magnets in TR_A and TR_B synchronously such that the condition $\Delta\tau_B = 2\Delta\tau_A$ remains satisfied. To ensure fulfilling of this criterion, the dependence of $\Delta\tau_B$ and $\Delta\tau_A$ on rotation of the magnets has been calibrated independently. The desired $\Delta\tau_B$ and $\Delta\tau_A$ can thus be obtained by rotating the magnets by the appropriate angle according to the calibration.

The temporal profiles of transmitted THz waves with different $\Delta\tau_A$ are shown in Fig. 3. The temporal THz profile is split from one peak into four peaks after passing through the filter. The equal time difference, $\Delta\tau_A$, between each peak can be observed from measured data. The transmitted frequency spectrum comes from the interference of these four parts of the THz signal and can be obtained by applying fast Fourier transform to the signals. The peak transmitted frequencies versus $\Delta\tau_A$ are shown in Fig. 4. The solid line is the theoretical curve according to $\Delta\tau_A \cdot f = 1$. The peak transmis-

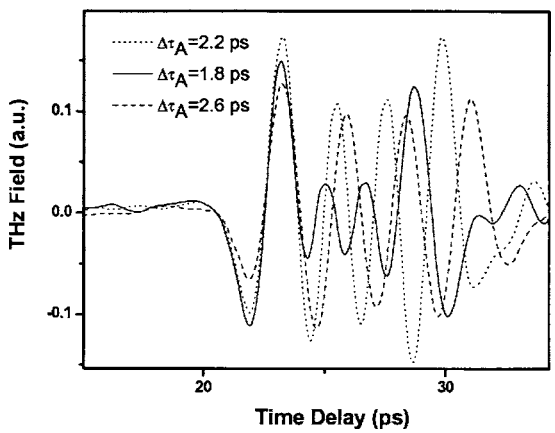

FIG. 3. THz signals transmitted through the tunable LC Lyot filter for delays, $\Delta\tau_A = 1.8$, 2.2 and 2.6 ps.

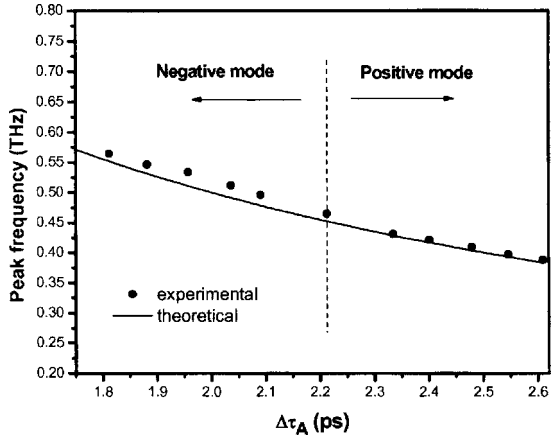

FIG. 4. The peak transmitted frequencies of the filter vs $\Delta\tau_A$. The circles are experimental data and the curve is theoretical prediction from Eq. (3).

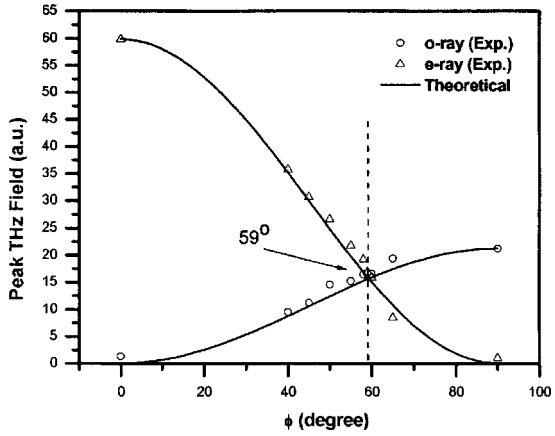

FIG. 5. The amplitudes of transmitted THz fields of e ray and o ray vs ϕ.

sion frequency of the filter decreases with the increasing $\Delta\tau_A$. The tuning range of the filter is from 0.388 to 0.564 THz. The insertion loss of the device is around 8 dB. It is attributed mainly to the scattering of the LC molecules of the thick cells (4.5 and 9 mm) used as fixed retarders.

Consider the case of a general Lyot filter consisting of a phase retarder between a pair of the parallel polarizers. The angle, ϕ, between the slow axis of the retarder and the polarization direction of the polarizers, will affect the ratio of the field amplitudes of e ray and o ray without changing the retardation. As the peak transmitted frequency of the Lyot filter depends only on the retardation [see Eq. (1)], the spectral distribution of electromagnetic wave transmitted trough the Lyot filter is not affected by the angle ϕ. On the other hand, the transmitted waves can be viewed as the interference of e ray and o ray propagating through the elements. Complete interference will only occur when the field amplitudes of the e ray and o ray are equal. In general, this condition can be achieved when $\phi=45°$ for a lossless retarder. The absorption of E7 ($\kappa<0.05$) in THz range is small.[18] The major losses in this work are scattering loss which is due to the thermal fluctuation of LC molecular orientations.[25] Further, the loss of ordinary ray is larger than that of the extraordinary ray in E7.

We have measured the peak amplitude of the transmitted THz electric fields for o ray and e ray as a function of ϕ. The experimental data are shown as open circles and triangles in Fig. 5, respectively. Recall that the electric field amplitudes of o ray and e ray, $E_o(\phi)$ and $E_e(\phi)$, are linearly proportional to $\sin^2(\phi)$ and $\cos^2(\phi)$, respectively. These are plotted a that solid curves in Fig. 5. Both the theoretical predictions and experimental data show that the ratio of $E_o(\phi)$ and $E_e(\phi)$ is indeed equal to 1 when $\phi=59°$.

In summary, we have demonstrated for the first time a tunable room-temperature THz Lyot filter. The key elements are fixed and variable liquid crystal phase retarders. The central bandpass frequency of the filter can be continuously tuned from 0.388 to 0.564 THz (a fractional tuning range of 40%) using magnetically controlled birefringence in nematic liquid crystals. The insertion loss of ~8 dB is attributed to scattering of the LC molecules in the thick LC cells. The bandwidth of the present device is 0.1 THz. Still narrower bandwidth is possible by adding more elements. This filter can be operated at room temperature. The experimental results are in agreement with theoretical predictions. Extension of the LC-based Lyot filter to the higher THz frequency range (10–30 THz) or mid-infrared is straightforward, with additional benefits of still larger tunable range because of the shorter wavelength.

This work was supported in part by the National Science Council (NSC) of R.O.C. under Grant No. NSC 93-2115-E-009-065 and the Program for the Pursuit of Academic Excellence of the Ministry of Education and NSC, R.O.C.

[1] *Sensing with Terahertz Radiation*, edited by D. Mittleman (Springer, Berlin, 2003).
[2] P. H. Siegel, IEEE Trans. Microwave Theory Tech. **50**, 910 (2002).
[3] B. Ferguson and X.-C. Zhang, Nat. Mater. **1**, 26 (2002).
[4] T. K. Wu, *Frequency Selective Surface and Grid Array* (Wiley, New York, 1995).
[5] C. Winnewisser, F. T. Lewen, M. Schall, M. Walther, and H. Helm, IEEE Trans. Microwave Theory Tech. **48**, 744 (2000).
[6] S. Biber, A. Hofmann, R. Schulz, M. Collischon, J. Weinzierl, and L. P. Schmidt, IEEE Trans. Microwave Theory Tech. **52**, 2183 (2004).
[7] D. M. Wu, N. Fang, C. Sun, X. Zhang, W. J. Padilla, D. N. Basov, D. R. Smith, and S. Schultz, Appl. Phys. Lett. **83**, 201 (2003).
[8] I. H. Libon, S. Baumgärtner, M. Hempel, N. E. Hecker, J. Feldmann, M. Koch, and P. Dawson, Appl. Phys. Lett. **76**, 2821 (2000).
[9] T. D. Drysdale, I. S. Gregory, C. Baker, E. H. Linfield, W. R. Tribe, and D. R. S. Cumming, Appl. Phys. Lett. **85**, 5173 (2004).
[10] H. Nemec, P. Kuzel, L. Duvillaret, A. Pashkin, M. Dressel, and M. T. Sebastian, Opt. Lett. **30**, 549 (2005).
[11] F. Yang and J. R. Sambles, Appl. Phys. Lett. **79**, 3717 (2001).
[12] M. Tanaka and S. Sato, Jpn. J. Appl. Phys., Part 1 **40**, 4131 (2001).
[13] C.-L. Pan, C.-F. Hsieh, R.-P. Pan, M. Tanaka, F. Miyamaru, M. Tani, and M. Hangyo, Opt. Express **13**, 3921 (2005).
[14] B. Lyot, Ann. Astrophys. **7**, 31 (1944).
[15] B. H. Billings, J. Opt. Soc. Am. A **37**, 738 (1947).
[16] W. I. Kaye, US Patent No. 4,394,069 (19 July 1983).
[17] C.-Y. Chen, T.-R. Tsai, C.-L. Pan, and R.-P. Pan, Appl. Phys. Lett. **83**, 4497 (2003).
[18] C.-Y. Chen, C.-F. Hsieh, Y.-F. Lin, R.-P. Pan, and C.-L. Pan, Opt. Express **12**, 2625 (2004).
[19] T.-R. Tsai, C.-Y. Chen, C.-L. Pan, R.-P. Pan, and X.-C. Zhang, Appl. Opt. **42**, 2372 (2003).
[20] R.-P. Pan, T.-R. Tsai, C.-Y. Chen, C.-H. Wang, and C.-L. Pan, Mol. Cryst. Liq. Cryst. **409**, 137 (2003).
[21] M. Nakamura, J. Appl. Phys. **52**, 4561 (1981).
[22] F. J. Kahn, Appl. Phys. Lett. **22**, 386 (1973).
[23] P. G. de Gennes and J. Prost, *The Physics of Liquid Crystals*, 2nd ed. (Oxford, New York, 1983).
[24] S. Nashima, O. Morikawa, K. Takata, and M. Hangyo, J. Appl. Phys. **90**, 837 (2001).
[25] W. T. Coffey and Y. P. Kalmykov, Liq. Cryst. **14**, 1227 (1993).